Quantitative Z-contrast imaging in the scanning transmission electron microscope with size-selected clusters

Z. W. Wang,[1] Z. Y. Li,[1,*] S. J. Park,[1] A. Abdela,[1] D. Tang,[2] and R. E. Palmer[1]

[1]*Nanoscale Physics Research Laboratory, School of Physics and Astronomy, University of Birmingham, Birmingham B15 2TT, UK*

[2]*FEI Company, Achtseweg Noord 5, 5651 GG Eindhoven, The Netherlands*

(Received 11 July 2011; published 26 August 2011)

This paper describes a new approach of quantification of annular-dark-field or *Z*-contrast image intensity as a function of inner acceptance angle of the detector in a scanning transmission electron microscope. By using size-selected nanoclusters of Pd ($Z = 46$) and Au ($Z = 79$), it is shown experimentally that the exponent in the power law $I \sim Z^{\alpha}$ varies strongly between 1.2 and 1.8 as the collection angle changes from 14 to 103 mrad. The result is discussed in line with existing theoretical models. Factors, such as cluster size, structure, and orientation as well as the detector geometry, are also discussed for potential use of the work.

DOI: 10.1103/PhysRevB.84.073408 PACS number(s): 36.40.−c

With today's developments in nanoscience and technology, there is an increasing demand to correlate, in a quantitative way, chemical composition, structure, and property of materials with reduced dimension and size. For example, Serpell *et al*. showed recently that the design, synthesis, and understanding of industrial catalysts with improved selectivity could benefit from knowing internal structures and composition of core-shell bimetallic nanoparticles.[1] Similarly, examples have been seen in nanoalloyed AuAg particles with potential use of tunable optical properties.[2] Here, *Z*-contrast imaging in scanning transmission electron microscopy (STEM) are applied in obtaining chemical composition within nanoparticles.

The so-called *Z*-contrast imaging method originates from the strong dependence of STEM image intensity on atomic numbers of elements when the signals are collected by a high-angle annular dark-field (HAADF) detector.[3–5] In this case, as proposed by Howie in 1979, the signals are predominantly thermal scattered electrons, and coherence is largely reduced.[6] Since then, there have been many studies on the capabilities and limitation of *Z*-contrast imaging.[7–14] While there are a number of specimen-related factors that contribute to the image contrast, including not only atomic number, but also the specimen thickness, the crystal structure, and the crystal orientation, the geometry of annular detector also plays an important role. The dependence of *Z* contrast on the detector geometry was investigated theoretically by Hartel *et al*., who pointed out that, for thin objects, an analytical expression for the *Z* dependence of image intensity can be approximated by an exponential function of the form $I \sim Z^{\alpha}$, where α is smaller than 2 and in the range 1.6–1.9 for most cases.[11] This power law has been widely accepted by the materials and microscopy community, however, without being experimentally verified. For effective quantitative characterizations using *Z*-contrast imaging, it is advantageous to know the critical exponent α as a function of detector angles.

Zhu *et al*. pointed out from their combination of simulation and experimental work on $SrTiO_3$ crystals (∼10–50 nm thickness) that the dependence of the imaging contrast on collection angle varies with sample thickness,[15] while Klenov and Stemmer show experimentally for a 40-nm-thick $PdTiO_3$ film on a $SrTiO_3$ single crystal that the STEM intensity ratio of different elements is insensitive to changes of the inner angles of the detector above ∼20 mrad.[16] While there is no general consensus on this topic, a wide range of values of α (1.3–2) has been used in the literature,[17–27] often without a full evaluation of microscope conditions. This situation hinders wider applications of quantitative STEM in nanomaterials characterization.

The difficulties of measuring the value of α lie in accurate measurements of sample thickness inside a microscope. For example, the film thickness measurements for the $SrTiO_3$ sample in Ref. 16 show a difference of 25% when convergent beam electron diffraction and low-loss electron energy spectra were used. In this study, we take a new approach addressing this problem by using size-selected clusters of two elements having the same number of atoms and with distinct different atomic number, Au ($Z = 79$) and Pd ($Z = 46$). Here, the size of the preformed clusters can be controlled with an accuracy of 5% in terms of the number of atoms they contained. We have conducted a systematic investigation of the image contrast of the Au and Pd clusters, from which the value of α is obtained.

Soft-landed size-selected Pd and Au clusters were produced by a radio frequency magnetron sputtering, gas aggregation cluster beam source with a lateral time-of-flight mass filter ($M/\Delta M = 20$).[28–30] The quantitative STEM investigation was performed in an FEG 200 kV Tecnai F20 electron microscope fitted with a Fischione Model 3000 detector. In this study, the camera length was varied between 70 and 520 mm, corresponding to inner collection angles of the detector of 103 to 14 mrad and outer collection angles of 227 to 70 mrad. All STEM images were acquired under optimized focus conditions that approached the Scherzer focus when the maximum intensity/contrast criterion was used.[16] The images for quantitative analysis were as recorded, i.e. no image processing was performed.

Figure 1(a) displays a representative image taken from a sample of size-selected Pd clusters deposited on a carbon film support, in which the arrows mark examples of Pd_{147} and Pd_{309} clusters. Here, the subscripts denote the number of atoms comprising each cluster. The codeposition of clusters with two different sizes was to ensure minimization of experimental variables on quantitative analysis. Figure 1(b) shows the integrated intensity over the clusters as a function of cluster size after subtracting the background contribution.

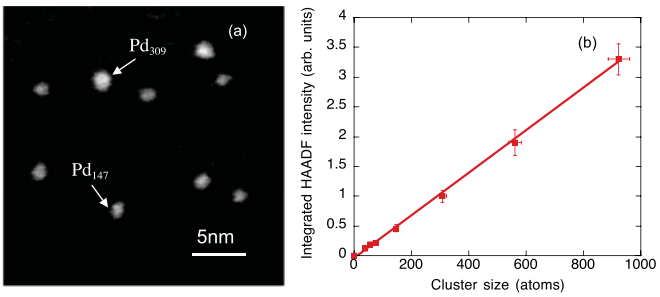

FIG. 1. (Color online) (a) Representative HAADF-STEM images of codeposited size-selected Pd clusters, Pd_{309} and Pd_{147} as indicated by arrows. (b) HAADF intensity integrated over Pd clusters as a function of cluster size. The error bars for intensity are the standard deviations from distributions of clusters with specified size, while the error bars for cluster size are from the mass resolution of the cluster source.

It is apparent that an approximately linear relationship exists between intensity and cluster size for up to 923 atoms (about 3 nm in diameter). In the shell model of an icosahedral structure, Pd_{923} corresponds to a maximum height of 13 atoms. This size regime is similar to that reported for Au

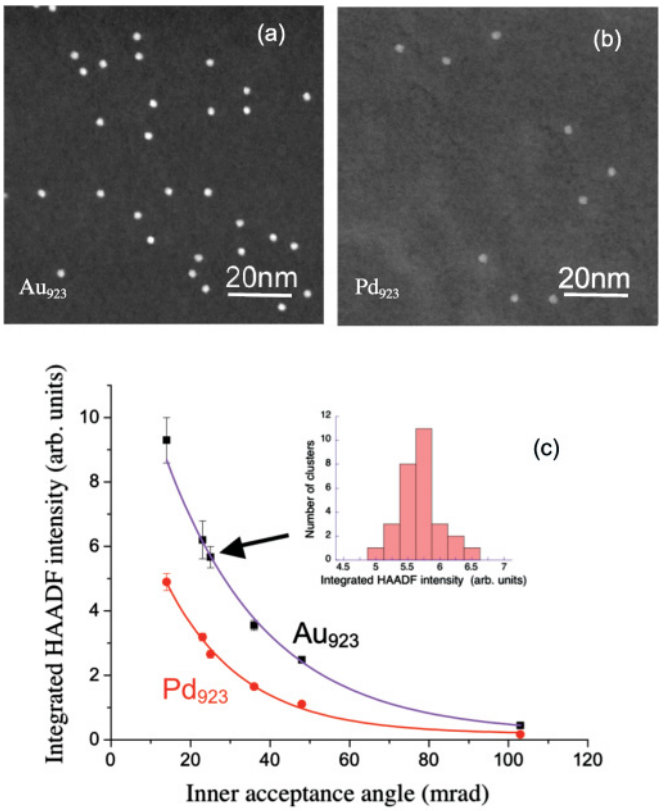

FIG. 2. (Color online) HAADF-STEM images for size-selected (a) Au_{923} and (b) Pd_{923} clusters, recorded with the same experimental conditions. The same greyscale settings (brightness/contrast) were used in both images. (c) The integrated HAADF intensity as a function of inner acceptance angle of the detector for size-selected Au_{923} and Pd_{923} clusters. The error bars are the standard deviations obtained from histograms of integrated STEM intensity of clusters, an example of which is shown for Au_{923}.

clusters previously,[31,32] suggesting that the linear mass-intensity relationship is not an element-specific physical property and that multiple scattering is not a dominant effect in this regime.

The above result is a platform for exploring the element-dependent STEM imaging contrast. STEM images were acquired by choosing a series of discrete camera lengths while keeping all other experimental conditions the same. Figures 2(a) and 2(b) present an example of the images of Au_{923} and Pd_{923} clusters when the smallest inner and outer collection angles (∼14 and 70 mrad, respectively) were used. Figure 2(c) displays the integrated HAADF intensity over each cluster as a function of the inner acceptance angle of the detector θ. No obvious intensity contrast reversal was observed here for all the acceptance angles used, suggesting contribution from the crystalline diffraction was limited.

By taking the ratio of integral intensity of Au and Pd clusters, one can evaluate the relationship between the exponent α and the angle θ, as shown in Fig. 3. It can be seen that the α increases monotonically with the inner acceptance angle and takes a value in the range 1.2–1.8 when θ varies from 14 to 103 mrad. The error bars were calculated from the propagation of square variance from the data in Fig. 2(c). The solid line shows that the data fit reasonably well to $\alpha = 2 - Ae^{B\theta}$, where A and B are fitting parameters. The residual of the least square fitting $R = 0.973$. It is noted that the result in Fig. 3 follows the trend shown by Hartel *et al.* from their theoretical model.[11] The α value smaller than 2 (the Coulomb limit) can be understood that, in practice, the nucleus charge of atoms is always partially shielded by bound electrons. The extrapolation (dashed line) of the curve in Fig. 3 suggests that a very large inner acceptance angle of the detector would be required in order to approach the true Rutherford scattering ($\alpha = 2$). Although the largest inner detector angle for Tecnai F20 is ∼140 mrad, our measurement was only conducted for the angle up to 103 mrad. This is due to the poor signal-to-noise ratio of clusters in HAADF imaging at this setting. As a result, the background noise from the carbon film support cannot be neglected. This is reflected in the larger error bar for the data point at 103 mrad. Here, we see that

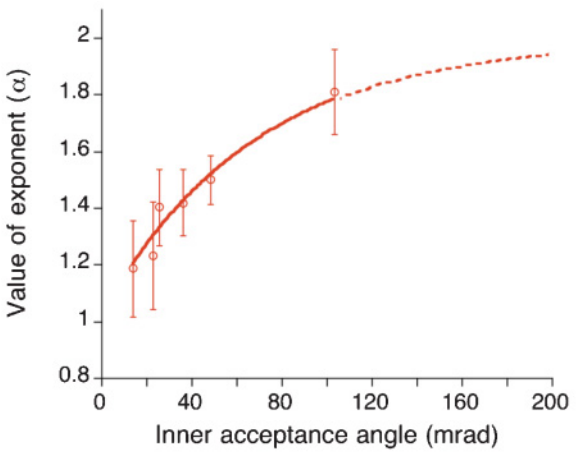

FIG. 3. (Color online) The value of the exponent α as a function of the inner acceptance angle, derived from Fig. 2(c) by assuming STEM intensity is proportional to Z^{α}. The dashed line represents the extrapolation of the curve fitted to the data points.

the required larger detector angle for incoherent imaging is in contradiction to the condition for minimum noise. Therefore, it is extremely useful that one knows the minimum tolerable inner detector angle for which Z^{α} relation is still valid. In practice, Z contrast has to be traded off against signal-to-noise ratio.

One also needs to be aware that electron scattering is a complex nonlinear process, especially for crystalline samples at zone axis. Therefore, simple analytical descriptions should be applied with caution. In Fig. 3, each data point is acquired by averaging intensity from a large number of supported clusters that are randomly oriented along the electron beam. Thus the contribution from the orientation-dependent diffraction contrast has been attenuated further in the present case. For potential use of this work in crystalline nanoparticles, in particular with aberration-corrected STEM, possible channeling effects need to be taken into account and be eliminated when possible.[33]

In summary, we have demonstrated a new approach of quantifying the imaging contrast in HAADF-STEM using size-selected clusters. We show that a linear relationship is obtained between the integrated HAADF intensity and cluster size for Pd clusters containing up to 923 atoms, consistent with the case of Au clusters, as previously reported. By comparing size-selected Au_{923} and Pd_{923} clusters, we have obtained the relationship between the exponent α in the Z^{α}-dependent HAADF intensity and the inner acceptance angle of the detector. These results allow us to determine quantitatively the local chemical composition without any additional spectroscopy techniques, as long as the global chemical information is known. With the current generation of aberration-corrected STEM, not only can we achieve higher spatial resolution, but also higher signal-to-noise ratio. We envisage that the use of size-selected clusters as a standard could enable an accurate determination of the chemistry of individual atomic columns in nanoparticles. There are a few examples having already demonstrated that Z-contrast imaging in STEM is now finding applications in exploration of quantitative materials characterization.[31,34,35] The Z-dependence relationship determined from our experiments should provide a valuable reference for future calculations and simulation work.

We thank the UK Engineering and Physical Science Research Council for financial supports.

*Z.Li@bham.ac.uk

[1]C. J. Serpell, J. Cookson, D. Ozkaya, and P. D. Beer, Nature Chemistry **3**, 478 (2011).
[2]Z. Y. Li, J. P. Wilcoxon, F. Yin, Y. Chen, R. E. Palmer, and R. L. Johnston, Faraday Discuss. **138**, 363 (2008).
[3]E. Zeitler and M. G. R. Thomson, Optik **31**, 359 (1970).
[4]A. V. Crewe, J. Wall, and J. Langmore, Science **168**, 1338 (1970).
[5]M. M. J. Treacy, A. Howie, and S. J. Wilson, Phil. Mag. A **38**, 569 (1978).
[6]A. Howie, J. Microscopy, **117**, 11 (1979).
[7]M. M. J. Treacy and S. B. Rice, J. Microscopy **156**, 211 (1989).
[8]R. F. Loane, P. Xu, and J. Silcox, Ultramicroscopy **40**, 121 (1992).
[9]J. Liu and J. M. Cowley, Ultramicroscopy **52**, 335 (1993).
[10]S. Hillyard and J. Silcox, Ultramicroscopy **58**, 6 (1995).
[11]P. Hartel, H. Rose, and C. Dinges, Ultramicroscopy **63**, 93 (1996).
[12]P. D. Nellist and S. J. Pennycook, Ultramicroscopy **78**, 111 (1999).
[13]A. Howie, Ultramicroscopy **98**, 73 (2004).
[14]D. A. Muller, Nat. Mater. **8**, 263 (2009).
[15]Y. M. Zhu, Hitatch E.M. News **2**, 2 (2009).
[16]D. O. Klenov and S. Stemmer, Ultramicroscopy **106**, 889 (2006).
[17]H. Lakner, C. Mendorf, B. Bollig, W. Prost, and F. J. Tegude, Mat. Sci. Eng. B **44**, 52 (1997).
[18]A. Singhal, J. C. Yang, and J. M. Gibson, Ultramicroscopy **67**, 191 (1997).
[19]C. P. Liu, R. D. Twesten, and J. M. Gibson, Ultramicroscopy **87**, 79 (2001).
[20]P. M. Voyles, J. L. Grazul, and M. A. Muller, Ultramicroscopy **96**, 251 (2003).
[21]M. Takeguchi, M. R. McCartney, and D. J. Smith, Appl. Phys. Lett. **84**, 2103 (2004).
[22]Z. Y. Li, J. Yuan, Y. Chen, R. E. Palmer, and J. P. Wilcoxon, Appl. Phys. Lett. **87**, 243103 (2005).
[23]Z. Y. Li, J. Yuan, Y. Chen, R. E. Palmer, and J. P. Wilcoxon, Adv. Mater. **17**, 2885 (2005).
[24]T. Walther, J. Microsc. **221**, 137 (2006).
[25]J. E. Allen, E. R. Hemesath, D. E. Perea, J. L. Lensch-Falk, Z. Y. Li, F. Yin, M. H. Gass, P. Wang, A. L. Beloch, R. E. Palmer, and L. Lauhon, Nature Nanotechnol. **3**, 168 (2008).
[26]M. Di Vece, S. Bals, J. Verbeeck, P. Lievens, and G. Van Tendeloo, Phys. Rev. B **18**, 125420 (2009).
[27]Z. W. Wang, O. Toikkanen, F. Yin, Z. Y. Li, B. M. Quinn, and R. E. Palmer, J. Am. Chem. Soc. **132**, 2854 (2010).
[28]I. M. Goldby, B. von Issendorff, L. Kuipers, and R. E. Palmer, Rev. Sci. Instrum. **68**, 3327 (1997).
[29]B. von Issendorff and R. E. Palmer, Rev. Sci. Instrum. **70**, 4497 (1999).
[30]S. Pratontep, S. J. Carroll, C. Xirouchaki, C. M. Streun, and R. E. Palmer, Rev. Sci. Instrum. **76**, 045103 (2005).
[31]Z. Y. Li, N. P. Young, M. Di Vece, S. Palomba, R. E. Palmer, A. L. Bleloch, B. C. Curley, R. L. Johnston, J. Jiang, and J. Yuan, Nature **451**, 46 (2008).
[32]N. P. Young, Z. Y. Li, Y. Chen, S. Palomba, M. Di Vece, and R. E. Palmer, Phys. Rev. Lett. **101**, 246103 (2008).
[33]C. Langlois, Z. W. Wang, D. Pearmain, C. Ricolleau, and Z. Y. Li, J. Phys: Conf. Ser. **241**, 012043 (2010).
[34]J. M. LeBeau, A. J. D'Alfonso, S. D. Findlay, S. Stemmer, and L. J. Allen, Phys. Rev. B. **80**, 174106 (2008).
[35]J. M. LeBeau, S. D. Findlay, L. J. Allen, and S. Stemmer, Nano Lett. **10**, 4405 (2010).